

# Electron and Neutron Electric Dipole Moments in the Focus Point Scenario of SUGRA Model

Utpal Chattopadhyay<sup>(a)</sup>, Tarek Ibrahim<sup>(b)</sup> and D.P. Roy<sup>(a)</sup>

<sup>(a)</sup>Department of Theoretical Physics

Tata Institute of Fundamental Research, Mumbai - 400 005, India

<sup>(b)</sup>Department of Physics, Faculty of Science  
University of Alexandria, Alexandria, Egypt

## Abstract

We estimate the electron and neutron electric dipole moments in the focus point scenario of the minimal SUGRA model corresponding to large sfermion masses and moderate to large  $\tan\beta$ . There is a viable region of moderate fine-tuning in the parameter space, around  $\tan\beta \simeq 5$ , where the experimental limits on these electric dipole moments can be satisfied without assuming unnaturally small phase angles. But the fine-tuning constraints become more severe for  $\tan\beta > 10$ .

PACS numbers: 04.65.+e, 12.60.Jv, 13.40.Em, 14.20.Dh

It has been long recognised that the experimental limits on the electron and neutron electric dipole moments (EDM) imply stringent constraints on the minimal supersymmetric standard model (MSSM) and in particular the minimal supergravity (SUGRA) model [1]. In order to satisfy these limits one has to assume either unnaturally small phase angles ( $< 10^{-2}$ ) in the model or multi-TeV superparticle masses [2]. More recently it has been shown by the authors of ref. [3] that the problem is alleviated to a large extent by internal cancellation between different supersymmetric (SUSY) contributions to these EDMs. Consequently, one can satisfy the experimental constraints on the EDMs with moderate phase angles and moderate superparticle masses in the unconstrained version of the MSSM [4, 5]. However one still requires large superparticle masses in the minimal SUGRA model [3, 6, 7], which is undesirable for three reasons. It implies, i) a large fine-tuning parameter for radiative breaking of electroweak symmetry, ii) a less viable SUSY signal at the forthcoming colliders, and iii) a very large dark matter density of the universe [7].

Recently, Feng, Matchev and Moroi [8] have pointed out that the radiative electroweak symmetry breaking condition and hence the resulting fine-tuning is practically independent of the universal soft scalar mass parameter  $m_0$  in the minimal SUGRA model for moderate to large values of  $\tan\beta$  ( $\gtrsim 5$ ). This is also the range favoured by the LEP data[9]. This has been referred to as the focus point phenomenon. It implies that one can have a  $m_0$  and hence sfermion masses of the first two generations in the multi-TeV region without affecting the fine-tuning parameter of electroweak symmetry breaking. Besides, one expects in this case an inverted hierarchy of squark masses, resulting in a distinctive SUSY signal at the LHC from gluino production [10, 11]. Moreover, it has been shown to predict a dark matter density of the universe, which is in fact in the desired range [12].

In this paper we have calculated the electron and neutron EDMs in the focus point scenario to see if they can be reconciled with the corresponding experimental limits without assuming unnaturally small phase angles. The large mass of the first generation sfermions in this model helps to suppress the electron and neutron EDMs. Moreover, a large value of the trilinear coupling parameter  $A_0$  helps to suppress them further via a more effective cancellation between the different SUSY contributions. But this is partly offset by the increase of these EDMs with  $\tan\beta$ . Thus for  $\tan\beta > 10$ , one cannot satisfy the experimental limits without assuming unnaturally small phase angles. However, there is a viable region of the parameter space at around  $\tan\beta \simeq 5$ , where the experimental limits can be satisfied with moderate values of the phase angles.

In the following section we briefly discuss the focus point scenario of the minimal SUGRA

model and estimate the fine-tuning parameter over the region of interest to the EDM calculation. In the next section we discuss the EDM calculation and identify the region of parameter space, where the EDMs can be reconciled with the experimental limits for moderate phase angles. We shall conclude with a brief summary of our results.

### Focus Point and Fine-tuning:

The basic parameters of the minimal SUGRA model are  $m_0, M_{1/2}, A_0, B$  and  $\mu$  – i.e. soft supersymmetry breaking scalar and gaugino masses, trilinear and bilinear couplings, along with the supersymmetric Higgs mass parameter [13]. The last two can be determined in terms of the two Higgs vacuum expectation values,  $v_1$  and  $v_2$ , using the two minimisation conditions. The first condition determines  $B$  in terms of the ratio  $v_2/v_1 \equiv \tan \beta$  and the sum

$$v^2 = v_1^2 + v_2^2 = 2m_Z^2/(g^2 + g'^2) \simeq 175 \text{ GeV}. \quad (1)$$

The second condition gives

$$\frac{1}{2}m_Z^2 = \frac{m_{H_1}^2 - m_{H_2}^2 \tan^2 \beta}{\tan^2 \beta - 1} - |\mu|^2 + \Delta_R, \quad (2)$$

where the last term comes from the radiative correction to the Higgs potential. This equation determines the modulus of  $\mu$ .

Thus for any  $\tan \beta$ , the naturalness of the electroweak symmetry breaking scale requires  $m_{H_2}^2$  and  $|\mu|^2$  to be of the order of  $m_Z^2$ , so that there is no large cancellation between these quantities [14]. Since  $m_{H_2}^2$  is linearly related to  $m_0^2, M_{1/2}^2$  and  $|A_0|^2$  via its renormalisation group equation (RGE), one usually assumes the naturalness criterion to imply each of these parameters to be  $< 1$  TeV. Indeed, most of the phenomenological studies within the minimal SUGRA model are based on this assumption. However, as pointed out by Feng et al [8], for physical values of the top quark mass and the gauge couplings,  $m_{H_2}^2$  at the electroweak scale becomes practically independent of its GUT scale value  $m_0^2$  for  $\tan \beta \gtrsim 5$ . One can see this result from the approximate analytic solution of the one-loop RGE for  $m_{H_2}^2$  [15, 16]. For  $\tan \beta$  not too large, one gets while neglecting the  $b$  Yukawa coupling contribution,

$$m_{H_2}^2 \simeq m_0^2 - \frac{3}{2}ym_0^2 + f(M_{1/2}, A_0, y), \quad (3)$$

Here  $f$  is a quadratic function of the soft parameters  $M_{1/2}$  and  $A_0$ , and  $y$  represents the top Yukawa coupling squared relative to its fixed point value, i.e.

$$y = \frac{h_t^2}{h_f^2} = \frac{1 + 1/\tan^2 \beta}{1 + 1/\tan^2 \beta_f}. \quad (4)$$

The top Yukawa coupling is related to its running mass,

$$h_t = m_t(M_t)/v \sin \beta, \quad (5)$$

which is related in turn to the physical top quark mass via

$$M_t = m_t(M_t) [1 + \Delta_{\text{QCD}} + \Delta_{\text{SUSY}}]. \quad (6)$$

The QCD and SUSY radiative corrections add about 6% and 4% respectively to the running mass to arrive at the physical top pole mass,  $M_t = 175 \pm 5$  GeV [9]. It is well known now that a physical top mass of 175 GeV corresponds to the fixed point value,  $\tan \beta_f \simeq 1.5$  at the electroweak scale [16], which defines the minimal value of  $\tan \beta$  in this model. Such a low value of  $\tan \beta$  is of course ruled out by the recent LEP limit on the lightest higgs boson mass [9], suggesting  $\tan \beta > 2(4)$  for maximal (small) stop mixing. Substituting the above value of  $\tan \beta_f$  in (4) gives

$$y \simeq 2/3 \text{ for } \tan \beta \gtrsim 5. \quad (7)$$

Thus over a large range of  $\tan \beta$ , which is also favoured by the above mentioned LEP data,  $m_{H_2}^2$  of eq. (3) at the electroweak scale is practically independent of its GUT scale value  $m_0^2$ . This is the so called focus point phenomenon, which implies that  $m_0$  can be made  $> 1$  TeV without affecting the naturalness criterion. The corresponding squark and slepton masses of the first two generations remain large at the electroweak scale,

$$m_{\tilde{q}, \tilde{l}}^2 \simeq m_0^2 + O(M_{1/2}^2) > 1 \text{ TeV}, \quad (8)$$

since their RGEs are not affected by the top Yukawa coupling. Interestingly, the focus point condition ensures that  $|\mu|^2$  at the electroweak scale is practically the same as its GUT scale value, since [16]

$$|\mu|^2 = 1.8|\mu_0|^2(1 - y)^{\frac{1}{2}} \simeq |\mu_0|^2. \quad (9)$$

The sensitivity of the electroweak scale to the SUSY parameters are determined from eq. (2) in terms of the partial derivatives

$$C_a = \left| \frac{a}{m_Z^2} \frac{\partial m_Z^2}{\partial a} \right|, \quad (10)$$

where  $a$  denotes  $m_0, M_{1/2}, \mu_0$  and  $A_0$ . The fine-tuning is defined by the largest of these quantities [14]

$$C = \max \{ C_{m_0}, C_{M_{1/2}}, C_{\mu_0}, C_{A_0} \}. \quad (11)$$

This parameter is a plausible though not unique measure of fine-tuning. It is based on the sensitivity of the electroweak scale to the SUSY parameters, but not other quantities like  $m_t$ [8].

For estimating the fine-tuning parameter we have taken the radiative electroweak symmetry breaking code of ref. [17], which uses two-loop RGEs along with two-loop QCD correction to the top quark mass of eq. (6); and added the one-loop SUSY correction to the latter following ref. [18]. The radiative correction to the Higgs potential in (2) is evaluated using the complete one-loop result [19].

We have computed the fine-tuning parameter  $C$  in the  $(m_0 - A_0)$  planes of Figs. (1a) to (1d) for fixed values of  $M_{1/2}$ . Figs. (1a) and (1b) show the contour plots of  $C$  for  $M_{1/2} = 300$  and 500 GeV at  $\tan\beta = 5$ , while Figs. (1c) and (1d) show the analogous plots at  $\tan\beta = 10$ . The phases in these figures correspond to  $\phi_\mu = 0$ , and  $\phi_{A_0} = 0$  and  $\pi$ , for the upper and the lower half regions of the contours respectively. In general,  $C$  is very weakly sensitive to the phase  $\phi_\mu$  as long as  $\phi_\mu$  is in a range which satisfies the EDM constraints in a broad region of parameter space. On the other hand, it is modestly sensitive to the phase  $\phi_{A_0}$  as can be seen by comparing the  $\phi_{A_0} = 0$  and  $\pi$  parts of the contours in Figs. (1a) to (1d).

We see that for moderate values of  $|A_0|$  ( $< 2000$  GeV) the fine-tuning parameter increases appreciably with  $M_{1/2}$ , but it is effectively independent of  $m_0$  at fixed  $M_{1/2}$  and  $A_0$ . Figs. (1a) and (1b) indicate that, for contours with  $\phi_{A_0} = 0$ , one can go up from  $A_0 \simeq m_0 \simeq 0$  to  $m_0 \simeq 2000$  GeV and  $A_0 \simeq 1500$  GeV without paying any appreciable price in terms of fine-tuning. Finally, these figures also show that there is only a marginal improvement of the fine-tuning parameter in increasing  $\tan\beta$  from 5 to 10.

### EDMs of Electron and Neutron:

The EDM of an elementary fermion (electron or quark) is the coefficient  $d^f$  of the effective Lagrangian

$$\mathcal{L}_E = \frac{-i}{2} d^f \bar{\psi} \sigma_{\mu\nu} \gamma_5 \psi F^{\mu\nu}, \quad (12)$$

which has the nonrelativistic limit  $d_f \psi_A^\dagger \vec{\sigma} \cdot \vec{E} \psi_A$ ,  $\psi_A$  being the large component of the Dirac field. Fig. (2) shows the one-loop contributions to the effective Lagrangian of eq. (12) in the MSSM, coming from the chargino and the neutralino exchanges, along with the gluino exchange in the case of quark. Denoting the generic interaction Lagrangian by

$$- \mathcal{L}_{int} = \sum_{ik} \bar{\psi}_f (K_{ik} P_L + L_{ik} P_R) \psi_i \phi_k + \text{H.C.}, \quad (13)$$

the one-loop EDM is given by [3]

$$d^f = \sum_{ik} \frac{m_i}{(4\pi)^2 m_k^2} \text{Im}(K_{ik} L_{ik}^*) \left[ Q_i A \left( \frac{m_i^2}{m_k^2} \right) + Q_k B \left( \frac{m_i^2}{m_k^2} \right) \right], \quad (14)$$

where  $P_{L,R} = (1 \mp \gamma_5)/2$  and

$$A(r) = \frac{1}{2(1-r)^2} \left( 3 - r + \frac{2\ell nr}{1-r} \right), \quad B(r) = \frac{1}{2(1-r)^2} \left( 1 + r + \frac{2r\ell nr}{1-r} \right). \quad (15)$$

Here  $Q$  denotes electric charge. The  $Q_i$  and  $Q_k$  terms in (14) correspond to the diagrams with photon coupling to the chargino  $\chi_i^\pm$  and the sfermion  $\tilde{f}_k$  respectively.

The presence of CP violating phases in the minimal SUGRA model is responsible for a nonzero imaginary part for the product  $K_{ik} L_{ik}^*$  in (14). If one neglects sfermion flavour mixing to avoid large flavour changing neutral current effects, then there are two independent physical CP violating phases in this model [20]. They can be chosen to be the phases of  $\mu$  and  $A_0$ , namely  $\phi_\mu$  and  $\phi_{A_0}$ , while  $M_{1/2}$  and  $B\mu$  are chosen to be real [3, 6, 7]. The reality of  $B\mu$  ensures that the Higgs vacuum expectation values and the resulting  $\tan\beta$  are real. Following the renormalisation group equation of  $\mu$  one may note that the phase of  $\mu$  is scale independent.

The form of the effective Lagrangian of eq. (12) requires different chiralities of the initial and the final state fermions, as indicated in Fig. (2) and eq. (14). For the gluino exchange contribution, this comes from the chirality flip of the sfermion via the  $L$ - $R$  mixing term in its mass squared matrix. For the chargino exchange contribution, this is accomplished via gaugino-higgsino mixing in the  $\chi^\pm$  mass matrix, while the sfermion preserves its chirality. The neutralino exchange receives contribution from both of these sources. Since both the  $L$ - $R$  mixing sfermion mass squared term and the higgsino-sfermion-fermion coupling are proportional to  $m_f$ , all the contributions are proportional to the external fermion mass. Another consequence of the chirality flip is the explicit proportionality of the contributions to the exchanged fermion mass  $m_i$  in eq. (14).

The gluino exchange contribution to the quark EDM is given by

$$d_{\tilde{g}}^q = -\frac{2e\alpha_s}{3\pi} \sum_{k=1}^2 \text{Im}(D_{2k}^q D_{1k}^{q*}) \frac{m_{\tilde{g}}}{M_{\tilde{q}_k}^2} Q_{\tilde{q}} B \left( \frac{m_{\tilde{g}}^2}{M_{\tilde{q}_k}^2} \right), \quad (16)$$

where  $D^q$  is the  $L$ - $R$  mixing matrix for the squark  $\tilde{q}$ , which diagonalises the corresponding  $M_{\tilde{q}}^2$  [3].

$$\text{Im}(D_{21}^q D_{11}^{q*}) = -\text{Im}(D_{22}^q D_{12}^{q*}) = \frac{m_q}{M_{\tilde{q}_1}^2 - M_{\tilde{q}_2}^2} (|A_q| \sin\phi_q + |\mu| \sin\phi_\mu R_q), \quad (17)$$

where

$$R_u = \cot \beta, \quad R_d = \tan \beta, \quad (18)$$

and  $\phi_q$  is the phase of  $A_q$  at the electroweak scale. For the first generation of fermions, the magnitudes and phases of the  $A$  parameters at the electroweak scale are close to those of  $A_0$  at large  $A_0$ , since [6]

$$\begin{aligned} A_u &\simeq (1 - 0.5y)A_0 - 2.8M_{1/2} \\ A_d &\simeq A_0 - 3.6M_{1/2} \\ A_e &\simeq A_0 - 0.7M_{1/2}. \end{aligned} \quad (19)$$

The chargino exchange contributions to the EDMs are given by

$$d_{\chi^+}^u \simeq \frac{-e\alpha m_u}{4\sqrt{2}\pi m_W \sin^2 \theta_W \sin \beta} \sum_{i=1}^2 \text{Im}(V_{i2}^* U_{i1}^*) \frac{m_{\chi_i^+}}{M_{\tilde{d}_1}^2} \left[ A \left( \frac{m_{\chi_i^+}^2}{M_{\tilde{d}_1}^2} \right) - \frac{1}{3} B \left( \frac{m_{\chi_i^+}^2}{M_{\tilde{d}_1}^2} \right) \right], \quad (20)$$

$$d_{\chi^+}^d \simeq \frac{-e\alpha m_d}{4\sqrt{2}\pi m_W \sin^2 \theta_W \cos \beta} \sum_{i=1}^2 \text{Im}(U_{i2}^* V_{i1}^*) \frac{m_{\chi_i^+}}{M_{\tilde{u}_1}^2} \left[ -A \left( \frac{m_{\chi_i^+}^2}{M_{\tilde{u}_1}^2} \right) + \frac{2}{3} B \left( \frac{m_{\chi_i^+}^2}{M_{\tilde{u}_1}^2} \right) \right], \quad (21)$$

$$d_{\chi^+}^e \simeq \frac{e\alpha m_e}{4\sqrt{2}\pi m_W \sin^2 \theta_W \cos \beta} \sum_{i=1}^2 \text{Im}(U_{i2}^* V_{i1}^*) \frac{m_{\chi_i^+}}{M_{\tilde{\nu}_e}^2} A \left( \frac{m_{\chi_i^+}^2}{M_{\tilde{\nu}_e}^2} \right), \quad (22)$$

where  $\tilde{u}_1, \tilde{d}_1$  refer to the dominantly left-handed squark mass eigenstates. In our numerical analysis we have also included the small contributions from the terms with  $\tilde{u}_2, \tilde{d}_2$ . Here,  $U$  and  $V$  are the gaugino-higgsino mixing matrices, which diagonalise the chargino mass matrix. Explicit expression for the  $U$  and  $V$  matrices are given in ref. [3] in terms of  $M_{1/2}$ ,  $\tan \beta$ ,  $|\mu|$  and  $\phi_\mu$ . We shall simply note here that each of the coefficients  $\text{Im}(U_{i2}^* V_{i1}^*)$  and  $\text{Im}(V_{i2}^* U_{i1}^*)$ , is proportional to  $|\mu| \sin \phi_\mu$ . Consequently,

$$d_{\chi^+}^{u,d,e} \propto |\mu| \sin \phi_\mu. \quad (23)$$

The neutralino exchange contributions to the EDMs can be collectively expressed as,

$$d_{\chi_0}^f = \frac{e\alpha}{4\pi \sin^2 \theta_W} \sum_{k=1}^2 \sum_{i=1}^4 \text{Im}(\eta_{ik}^f) \frac{m_{\chi_i^0}}{M_{f_k}^2} Q_{\tilde{f}} B \left( \frac{m_{\chi_i^0}^2}{M_{f_k}^2} \right), \quad (24)$$

where

$$\begin{aligned} \eta_{ik}^f &= \left[ -\sqrt{2} \{ \tan \theta_W (Q_f - T_{3f}) N_{1i} + T_{3f} N_{2i} \} D_{1k}^{f*} - \kappa_f N_{bi} D_{2k}^{f*} \right] \\ &\times \left( \sqrt{2} \tan \theta_W Q_f N_{1i} D_{2k}^f - \kappa_f N_{bi} D_{1k}^f \right), \end{aligned} \quad (25)$$

with

$$\kappa_u = \frac{m_u}{\sqrt{2}m_W \sin \beta}, \quad \kappa_{d,e} = \frac{m_{d,e}}{\sqrt{2}m_W \cos \beta} \quad (26)$$

and  $b = 4(3)$  for  $u(d, e)$ . The  $D^f$  are the  $L$ - $R$  mixing matrices for the sfermion  $\tilde{f}$ , which occurred earlier in eq. (16). Explicit expression for its matrix elements are given in ref. [3] in terms of  $|A_f|$ ,  $|\mu|$ ,  $\phi_f$  and  $\phi_\mu$ . Finally,  $N$  is the  $4 \times 4$  unitary matrix, diagonalising the neutralino mass matrix, which is evaluated numerically.

The main contributions to the EDM of quarks come from chargino and gluino exchanges, while neutralino exchange contribution is relatively small. They are related to the neutron EDM via the nonrelativistic quark model relation [21],

$$d^n = \frac{1}{3} [4d^d - d^u] \eta_E, \quad (27)$$

where  $\eta_E = 1.53$  is a QCD correction factor for evolving down the quark EDMs from the electroweak to the hadronic scale [3, 22].

There are two other contributions to the neutron EDM, arising from the quark chromoelectric dipole moment and the gluonic dimension-six operator, which are defined by the effective Lagrangians

$$\mathcal{L}'_E = \frac{-i}{2} d_C^q \bar{q} \sigma_{\mu\nu} \gamma_5 T^a q G^{\mu\nu a} \quad (28)$$

and

$$\mathcal{L}''_E = -\frac{1}{6} d_G f_{abc} G_{\mu\nu a} G_b^{\nu\rho} \tilde{G}_{\rho c}^\mu, \quad (29)$$

where  $T^a$  are the  $SU(3)$  generators,  $f_{abc}$  the Gell-Mann coefficients and  $G^{\mu\nu a}$  the gluonic field tensors [23]. Their contributions to the neutron EDM were earlier supposed to be small with respect to the quark EDM contribution of eq. (27) [22]. But as demonstrated in ref. [3], the large internal cancellation between the chargino and the gluino contributions to the  $d^q$  can make the net quark EDM contribution comparable to those from the quark chromoelectric and the gluonic dimension-six operators over certain regions of parameter space. In the present analysis we have included each of these three contributions to the neutron EDM following ref. [3].

We have investigated the ranges of the phase angles  $\phi_\mu$  and  $\phi_{A_0}$ , over which the predicted electron and neutron EDMs can be reconciled with the corresponding experimental limits [9],

$$d^e < 4.3 \times 10^{-27} \text{ ecm}, \quad d^n < 6.3 \times 10^{-26} \text{ ecm}. \quad (30)$$

It may be noted here that the above neutron EDM limit is a factor of 2 smaller than that considered in most of the previous analyses [3, 5, 6, 7]. Although it is still an order of



magnitude larger than the electron EDM, both of these provide comparable constraints over the parameter space of interest in our analysis.

Figs. (3a), and (3b) show the range of  $\phi_\mu$  at  $\tan\beta = 5$ , over which the predicted electron and neutron EDMs can be reconciled with the experimental limits (30), by allowing a variation of  $\phi_{A_0}$  over the range of  $-\pi$  to  $\pi$ . It should be mentioned here that the chargino contribution to  $d^n$  or  $d^e$  overshoots the corresponding experimental limits for the moderate values of  $|\phi_\mu|$  ( $\sim 0.1 - 0.2$  radian) shown in Figs. (3a) and (3b). What helps to satisfy the experimental limits is a cancelling contribution from gluino exchange for  $d^n$  (and neutralino exchange for  $d^e$ ). Consequently, there is a strong correlation between the two phase angles, as noted in earlier analyses. In particular the maximal allowed value of  $|\phi_\mu|$  for a given  $m_0$  and  $|A_0|$  corresponds to  $|\phi_{A_0}| \sim \pi/2$ , and there is an opposite sign correlation between the phases. The relatively smaller range of  $\phi_\mu$  at moderate  $|A_0|$  ( $< 2000$  GeV) is due to a larger coefficient of  $\sin\phi_\mu$  in the chargino contribution of eq. (23) in comparison with the coefficient of  $\sin\phi_{A_0}$  in the gluino contribution coming from eqs. (16,17,19). It is seen that only for very large  $|A_0|$  ( $\geq 6000$  GeV) the two coefficients become comparable; and one can satisfy the experimental limits for any value of  $\phi_\mu$ . But, one has to pay a high price in terms of the fine-tuning parameter amounting to  $C > 1000$ . Besides, the purely gluonic dimension six operators play an effective role in the cancellation mechanism in this region.

It should be added here that in plotting Figs. (3a) to (3d) we have scanned the  $m_0$  space in 50 GeV bins. Decreasing the size of this bin further leads to occasional spikes in the maximum value of  $|\phi_\mu|$ . This is indeed an important effect reflecting further suppression of the neutron EDM due to internal cancellation amongst the electric dipole, chromoelectric dipole and the gluonic operator contributions. As already noted in ref. [3], such a drastic suppression of the EDM can occur over narrow ranges of the SUGRA parameters due to these cancellations. But in the present analysis we shall concentrate only on those results which hold over wide range of SUGRA parameters, granting a possible correlation between the two phases.

In Figs. (3a) and (3b) we have indicated the fine-tuning parameter  $C$  at some specific points on the fixed  $|A_0|$  contours. Essentially, the point marked on each contour corresponds to the region of the right tip of the fixed  $C$  contours for  $\phi_{A_0} = 0$  of Figs. (1a) and (1b). Comparing the two figures one can easily see that  $C$  hardly varies up to the marked point on each  $|A_0|$  contour. Thus one can accommodate at least moderate values of  $|\phi_\mu^{\max}| = 0.1 - 0.2$  radian for  $C = 100 - 200$ , i.e. without paying any price in term of fine-tuning. Figs. (3c) and (3d) show the analogous ranges of  $\phi_\mu$  at  $\tan\beta = 10$ . We see that for given values of

$|A_0|$ , corresponding to the similar values of  $C$ , the  $\phi_\mu$  range is less than half the size of that of Figs.(3a) or (3b). The underlying reason of course is the comparatively larger coefficients of the chargino contributions for  $d^d$  of eq. (21) and  $d^e$  of eq. (22) at large  $\tan\beta$ . Thus the EDM limits disfavour large values of  $\tan\beta$  ( $\geq 10$ ).

Finally, we also analyse the case of  $\tan\beta = 3$  and  $M_{1/2} = 300$  GeV, as displayed in Figs. (4a) and (4b). Fig. (4a) shows the contours for constant fine-tuning  $C$  which are very different from what we found in Fig. (1a). Such a low value of  $\tan\beta$  falls outside the focus point scenario [8]. Besides, it is disfavoured by the LEP limit on the lightest Higgs mass [9]. Nonetheless most of the previous EDM analyses have concentrated in this low  $\tan\beta$  region [3, 6, 7], since it corresponds to smaller coefficients of the chargino contributions of eqs. (21) and (22). However, in this region of  $\tan\beta$  the fine-tuning parameter  $C$  steadily increases with  $m_0$  unlike what one finds in the focus point scenario. Here,  $C$  is same as  $C_{\mu_0}$ ; and a contour of constant  $C_{\mu_0}$  is a part of an ellipse [17]. Fig. (4b) shows the variation of maximal  $|\phi_\mu|$  with  $m_0$  for various  $|A_0|$  values. Unlike Figs. (3a) to (3d),  $C$  increases here rapidly along the contours of constant  $|A_0|$ . Consequently, a  $|\phi_\mu^{\max}|$  of 0.1 radian would correspond to a fine-tuning measure  $C \simeq 200$ , which is larger than the value required at  $\tan\beta = 5$  (Fig. (3a)).

### Summary:

We have analysed the electron and neutron EDMs in the focus point scenario of the minimal SUGRA model along with the fine-tuning parameter. In this scenario the soft scalar mass  $m_0$  can go up to 2 TeV without affecting the fine-tuning parameter. Similarly, the trilinear coupling parameter can be increased from 0 to 1.5 TeV without any appreciable increase in fine-tuning. The large  $m_0$  values correspond to large masses for the 1st generation of sfermions which helps to suppress the one-loop SUSY contributions to the EDMs. Moreover, the large  $|A_0|$  corresponds to larger gluino (neutralino) contribution to quark (electron) EDM, which can cancel the chargino contribution more effectively. Therefore, one can satisfy the experimental limits of the electron and the neutron EDMs without assuming unnaturally small phases  $\phi_\mu$  and  $\phi_{A_0}$  for  $m_0$  and  $|A_0|$  values of  $\sim 2$  TeV each. But this is possible only for a moderate value of  $\tan\beta \simeq 5$ . The chargino contributions to the EDMs increase with  $\tan\beta$ , so that the experimental limits cannot be satisfied without assuming small  $|\phi_\mu|$  or a large fine-tuning parameter  $C$  for  $\tan\beta > 10$ . Since the completion of this work a general phenomenological analysis in the focus point scenario including the EDMs has appeared recently in ref. [24]. However the present work contains a more detailed treatment of this

issue.

U.C. and D.P.R. thank Probir Roy for helpful discussions.

## References

- [1] For review and reference to earlier works, see S.M. Barr and W.J. Marciano, in “CP-violation”, ed. C. Jarlskog, World Scientific, Singapore (1989); W. Bernreuther and M. Suzuki, Rev. Mod. Phys. 63, 313 (1991).
- [2] P. Nath, Phys. Rev. Lett. 66, 2565 (1991); Y. Kizukuvi and N. Oshimo, Phys. Rev. D45, 1806 (1992); D46, 3025 (1992).
- [3] T. Ibrahim and P. Nath, Phys. Lett. B418, 98 (1998); Phys. Rev. D57, 478 (1998).
- [4] T. Ibrahim and P. Nath, Phys. Rev. D58, 111301 (1998); Phys. Rev. D61, 093004 (2000).
- [5] M. Brhlik, G.J. Good and G.L. Kane, Phys. Rev. D59, 115004 (1999).
- [6] A. Bartl, T. Gajdosik, W. Porod, P. Stockinger and H. Stremnitzer, Phys. Rev. D60, 073003 (1999).
- [7] T. Falk and K.A. Olive, Phys. Lett. B439, 71 (1998).
- [8] J.L. Feng, K.T. Matchev and T. Moroi, Phys. Rev. D61, 075005 (2000); Phys. Rev. Lett. 84, 2322 (2000).
- [9] Review of Particle Properties, Euro. Phys. J. C15, 1 (2000).
- [10] U. Chattopadhyay, A. Datta, A. Datta, A. Datta and D.P. Roy, Phys. Lett. B493: 127 (2000).
- [11] B.C. Allanach, J.P.J. Hetherington, M.A. Parker and B.R. Webber, Journal of High Energy Phys. 0008, 017 (2000)
- [12] J.L. Feng, K.T. Matchev and F. Wilczek, Phys. Lett. B482, 388 (2000).
- [13] P. Nath, R. Arnowitt and A.H. Chamseddinne, Applied  $N = 1$  supergravity (World Scientific, Singapore, 1984); H.P. Niles; Phys. Rep. 110, 1 (1984); H.E. Haber and G.L. Kane, Phys. Rep. 117, 195 (1985).

- [14] R. Barbieri and G.F. Giudice, Nucl. Phys. B306, 63 (1988); G.W. Anderson and D.J. Castano, Phys. Rev. D52, 1693 (1995); Phys. Rev. D53, 2403 (1996); P. Ciafaloni and A. Strumia, Nucl. Phys. B494, 41 (1997).
- [15] M. Carena, M. Olechowski, S. Pokorski and C.E.M. Wagner, Nucl. Phys. B419, 213 (1994).
- [16] J.A. Casas, J.R. Espinosa and H.E. Haber, Nucl. Phys. B526, 3 (1998).
- [17] K.L. Chan, U. Chattopadhyay and P. Nath, Phys. Rev. D58, 096004 (1998).
- [18] J. Bagger, K. Matchev, D. Pierce and R. Zhang, Nucl. Phys. B491, 3 (1997).
- [19] R. Arnowitt and P. Nath, Phys. Rev. D46, 3981 (1992); V. Barger, M.S. Berger and P. Ohmann, Phys. Rev. D49, 4908 (1994).
- [20] M. Dugan, B. Grinstein and L. Hall, Nucl. Phys. B255, 413 (1985); R. Garisto and J.D. Wells, Phys. Rev. D55, 1611 (1997).
- [21] A. Manohar and H. Georgi, Nucl. Phys. B234, 189 (1984).
- [22] R. Arnowitt, J. Lopez and D.V. Nanopoulos, Phys. Rev. D42, 2423 (1990); R. Arnowitt, M. Duff and K. Stelle, Phys. Rev. D43, 3085 (1991).
- [23] S. Weinberg, Phys. Rev. Lett. 63, 2333 (1989); E. Braaten, C.S. Li and T.C. Yuan, Phys. Rev. Lett. 64, 1709 (1990); J. Dai, H. Dykstra, R.G. Leigh, S. Paban and D.A. Dicus, Phys. Lett. B237, 216 (1990).
- [24] J.L. Feng and K.T. Matchev, hep-ph/0011356.

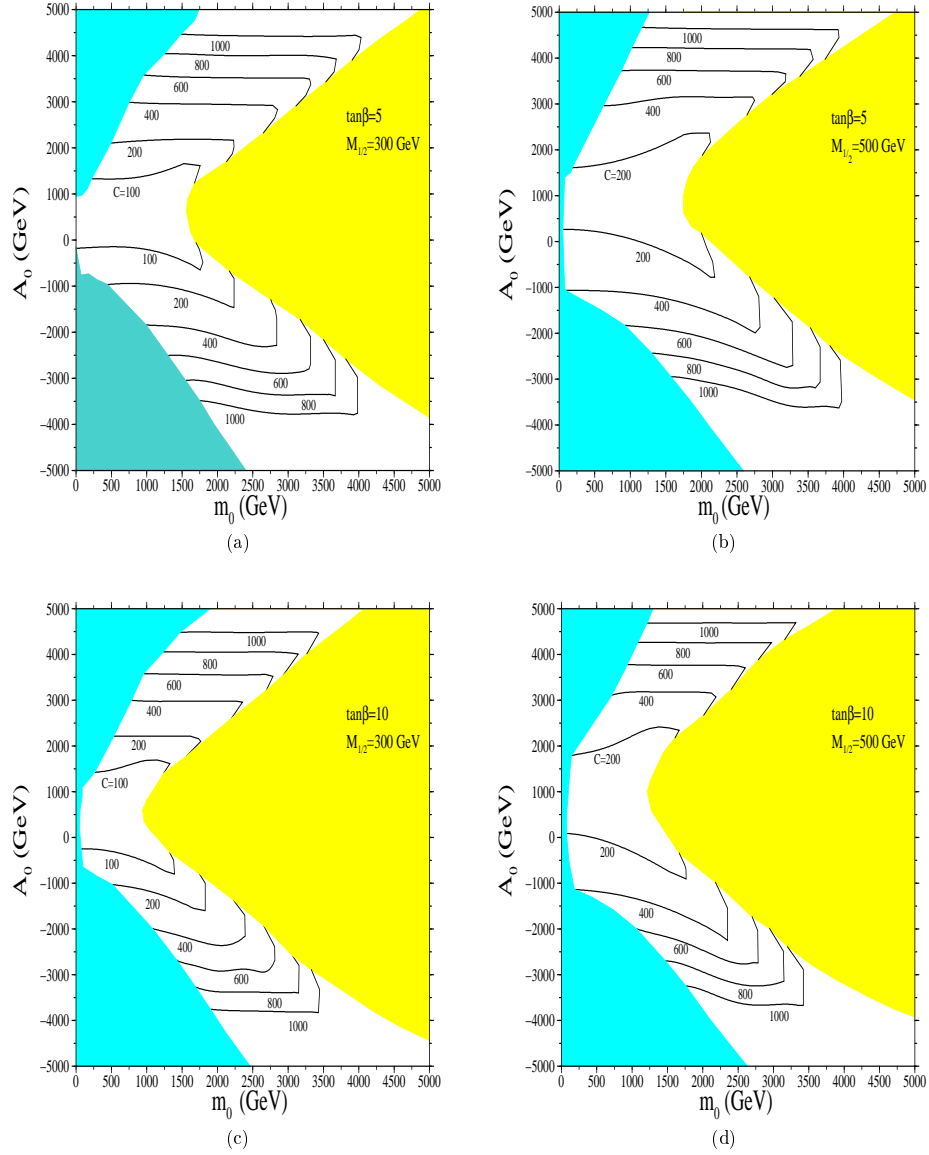


Figure 1: Lines of constant fine-tuning  $C$  in  $(m_0 - A_0)$  plane for different values of  $\tan\beta$  and  $M_{1/2}$ . Here  $\phi_\mu = 0$ , and for each contours  $\phi_{A_0}$  corresponds to 0 and  $\pi$  for the upper and the lower parts respectively. The shaded areas in the right represent the excluded regions due to the chargino mass limit and the electroweak radiative breaking constraint. The shaded areas in the left are excluded by the top squark mass bounds.

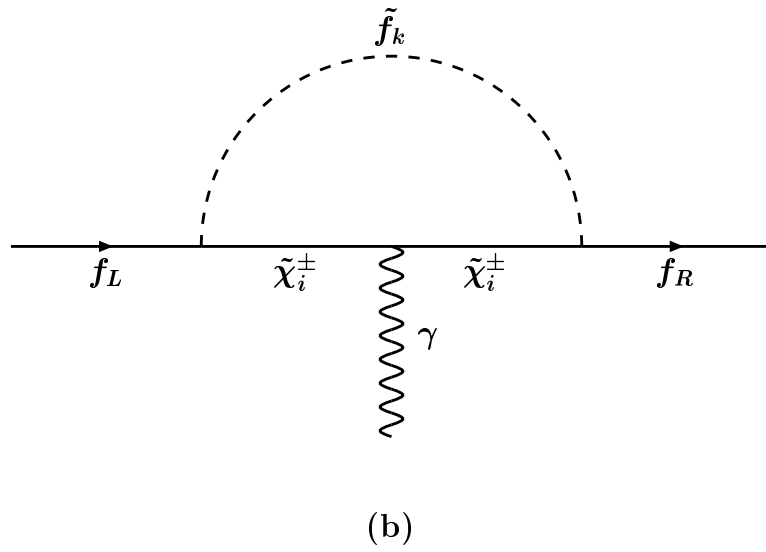
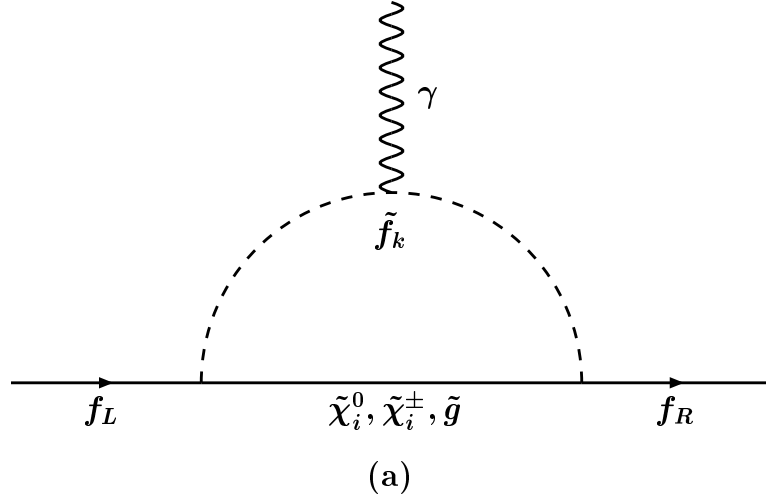


Figure 2: One loop diagrams contributing to the electric dipole moments of quarks and leptons.

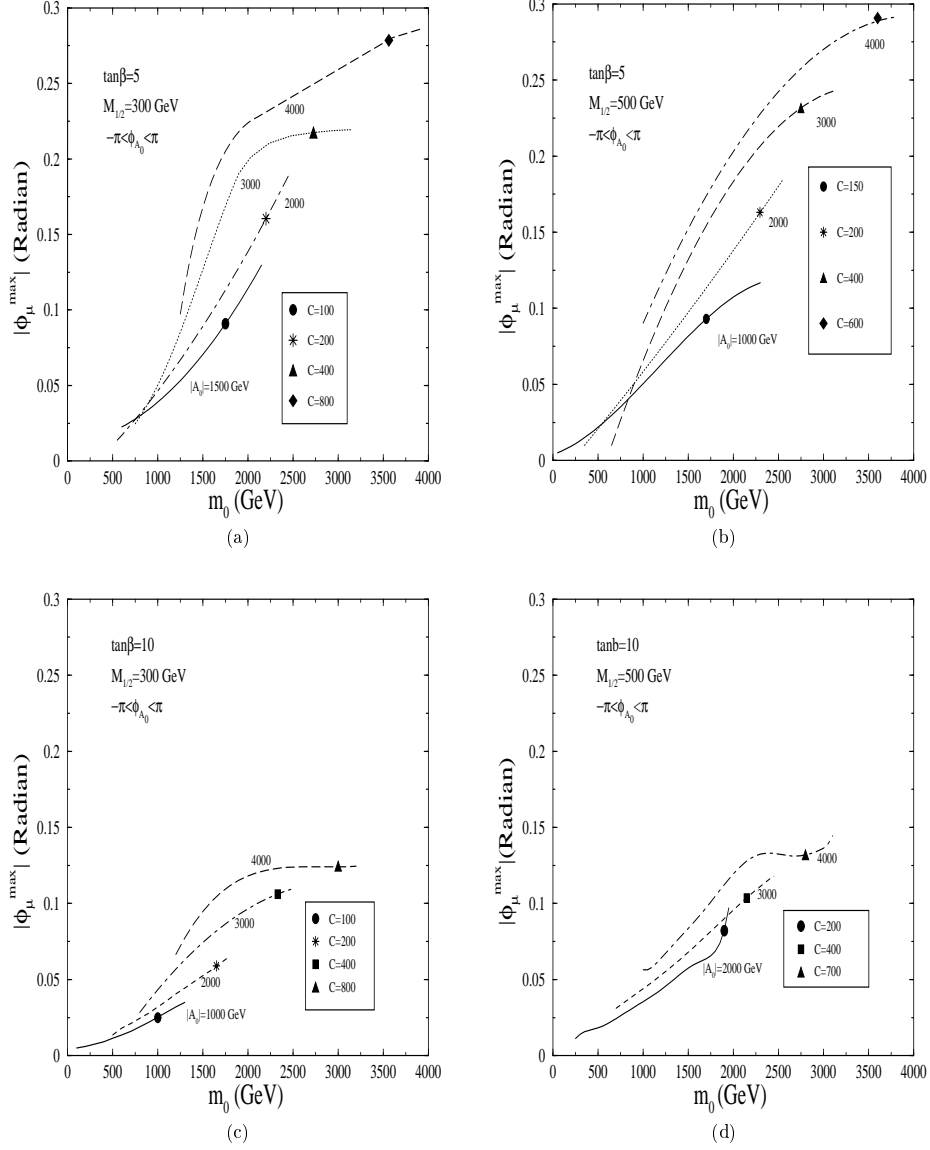


Figure 3: Lines of constant  $|A_0|$  in the plane of  $(|\phi_\mu^{max}| - m_0)$  for different cases of  $\tan\beta$  and  $M_{1/2}$ . Here the maximum value of  $|\phi_\mu|$  is obtained by varying  $\phi_{A_0}$  from  $-\pi$  to  $\pi$ . The symbols shown in the figures refer to the appropriate values of the fine-tuning measure  $C$  which remains practically constant on each curve up to the marked point.

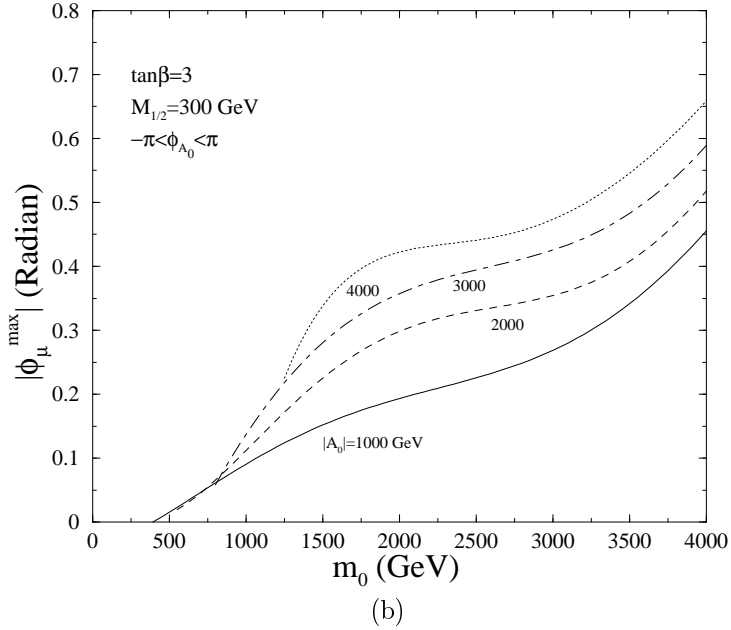
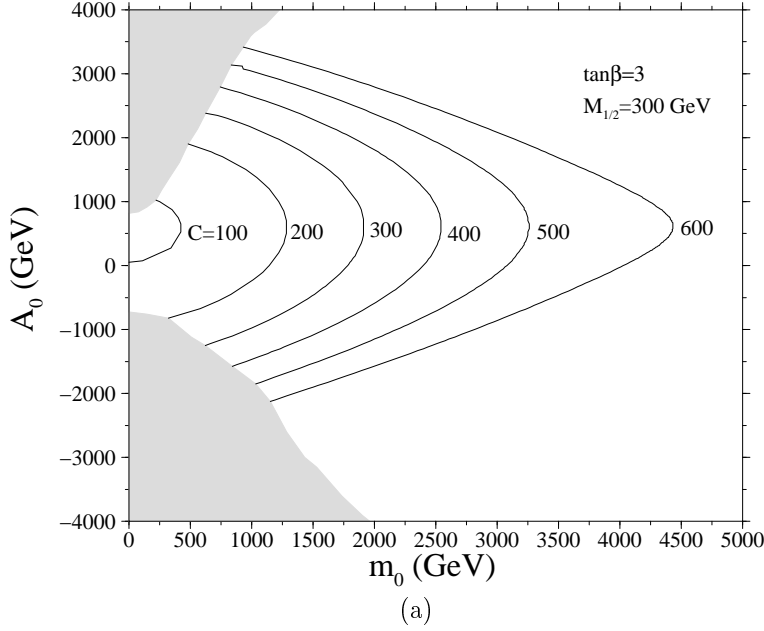


Figure 4: (a): Lines of constant fine-tuning  $C$  in  $(m_0 - A_0)$  plane for  $\tan\beta = 3$  and  $M_{1/2} = 300$  GeV. Here  $\phi_\mu = 0$ , and for each contours  $\phi_{A_0}$  corresponds to 0 and  $\pi$  for the upper and the lower parts respectively. The shaded areas in the left are excluded by the top squark mass bounds. (b): Lines of constant  $|A_0|$  in the plane of  $|\phi_\mu^{max}| - m_0$  for  $\tan\beta = 3$  and  $M_{1/2} = 300$  GeV. Here the maximum value of  $|\phi_\mu|$  is obtained by varying  $\phi_{A_0}$  from  $-\pi$  to  $\pi$ . Unlike Figs.(3a) to (3d), here  $C$  strongly varies along the constant  $|A_0|$  contours.